


# Anatomical Step-by-Step Dissection of Complex Skull Base Approaches for Trainees: Surgical Anatomy of the Endoscopic Endonasal Middle-Inferior Clivectomy, Odontoidectomy, and Far-Medial Approach

Edoardo Agosti<sup>1,2,3</sup> A. Yohan Alexander<sup>1,2</sup> Luciano C. P. C. Leonel<sup>1,2</sup> Jamie J. Van Gompel<sup>1,2,4</sup>   
Michael J. Link<sup>1,2,4</sup> Garret Choby<sup>1,2,4</sup> Carlos D. Pinheiro-Neto<sup>1,2,4</sup> Maria Peris-Celda<sup>1,2,4</sup>

<sup>1</sup>Rhodon Neurosurgery and Otolaryngology Surgical Anatomy Program, Mayo Clinic, Rochester, Minnesota, United States

<sup>2</sup>Department of Neurologic Surgery, Mayo Clinic, Rochester, Minnesota, United States

<sup>3</sup>Division of Neurosurgery, Department of Medical and Surgical Specialties, Radiological Sciences and Public Health, University of Brescia, Brescia, Italy

<sup>4</sup>Department of Otolaryngology/Head and Neck Surgery, Mayo Clinic, Rochester, Minnesota, United States

Address for correspondence Maria Peris-Celda, MD, PhD, Department of Neurologic Surgery and Otolaryngology, Rhodon Neurosurgery and Otolaryngology Surgical Anatomy Program, Mayo Clinic, 200 First Street, SW, Rochester, MN 55905, United States (e-mail: periscelda.maria@mayo.edu).

J Neurol Surg B Skull Base 2024;85:526–539.

## Abstract

### Keywords

- ▶ skull base surgery
- ▶ middle and inferior clivectomies
- ▶ odontoidectomy
- ▶ far-medial approach
- ▶ foramen lacerum
- ▶ pterygosphenoidal fissure

**Introduction** The clival, paraclival, and craniocervical junction regions are challenging surgical targets. To approach these areas, endoscopic endonasal trans-clival approaches (EETCAs) and their extensions (far-medial approach and odontoidectomy) have gained popularity as they obviate manipulating and working between neurovascular structures. Although several cadaveric studies have further refined these contemporary approaches, few provide a detailed step-by-step description. Thus, we aim to didactically describe the steps of the EETCAs and their extensions for trainees.

**Methods** Six formalin-fixed cadaveric head specimens were dissected. All specimens were latex-injected using a six-vessel technique. Endoscopic endonasal middle and inferior clivectomies, far-medial approaches, and odontoidectomy were performed.

**Results** Using angled endoscopes and surgical instruments, an endoscopic endonasal midclivectomy and partial inferior clivectomy were performed without nasopharyngeal tissue disruption. To complete the inferior clivectomy, far-medial approach, and partially remove the anterior arch of C1 and odontoid process, anteroinferior transposition of the Eustachian–nasopharynx complex was required by transecting pterygosphenoidal fissure tissue, but incision in the nasopharynx was not necessary. Full exposure of the craniocervical junction necessitated bilateral sharp incision and additional inferior mobilization of the posterior nasopharynx. Unobstructed access to neurovascular anatomy of the ventral posterior fossa and craniocervical junction was provided.

received

February 26, 2023

accepted after revision

June 19, 2023

accepted manuscript online

June 21, 2023

article published online

August 2, 2023

© 2023. Thieme. All rights reserved.  
Georg Thieme Verlag KG,  
Rüdigerstraße 14,  
70469 Stuttgart, Germany

DOI <https://doi.org/10.1055/a-2114-4660>.  
ISSN 2193-6331.

**Conclusion** EETCAs are a powerful tool for the skull-base surgeon as they offer a direct corridor to the ventral posterior fossa and craniocervical junction unobstructed by eloquent neurovasculature. To facilitate easier understanding of the EETCAs and their extensions for trainees, we described the anatomy and surgical nuances in a didactic and step-by-step fashion.

## Introduction

Surgically treating lesions of the clivus and surrounding structures is challenging.<sup>1-3</sup> While numerous approaches and trajectories have been effectively utilized, including retrosigmoid, transpetrosal, and anterior craniofacial, they may require extensive brain retraction and manipulation or extensive destruction of craniofacial structures and may not be ideal for certain pathologies.<sup>1,4-6</sup> Despite these extensive approaches, the surgeon is often operating between small windows by eloquent neurovascular structures.<sup>7-9</sup>

To reach the clivus, ventral jugular foramen, occipital condyle, and craniocervical junction, endoscopic endonasal transclival approaches (EETCAs) and their extensions have gained popularity as they provide excellent illumination and magnification, and a surgical trajectory ventral to the neurovasculature of the cerebellopontine angle.<sup>1,8-12</sup>

Although publications describing the EETCAs and their extensions are available, they often provide a general anatomical overview without didactic descriptions and illustrations of the steps involved in their execution.<sup>1,8-10,13-16</sup> Consequently, the main goal of this study is to develop an educational resource to help trainees understand the pertinent anatomy and procedural steps involved in safely and effectively performing the EETCAs and their extensions.

## Methods

All aspects of this study were approved by our Institutional Review Board and Biospecimens Committee, as required by standard protocols (17-005898).

Six cadaveric head specimens were dissected at the surgical anatomy laboratory at our institution. All specimens were formalin-fixed and latex-injected using a six-vessel technique.

A 0-degree and 30-degree endoscope (4 mm, 18 cm, Hopkins II, Karl Storz, Tuttlingen, Germany), attached to a high-definition camera and a digital video recorder system, was used together with a complete set of instruments for endoscopic endonasal skull base surgery. Following our dissections, the specimens were three-dimensional photo-documented with endoscopic techniques as previously described by our team.<sup>17</sup>

Endoscopic endonasal middle and inferior clivectomies, bilateral far-medial approaches, and odontoidectomy were modularly performed. Dissections were performed by one dissecting author (E.A.). Supervision was provided by the senior authors (M.P.C. and C.D.P.-N.) and a PhD in skull-base anatomy with advanced neuroanatomy experience (L.C.P.C.L.). Each

dissection was carried forward or repeated until the expected quality level was achieved so that each critical step was clearly documented.

Following successful dissection, representative cases were reviewed to emphasize basic principles of approach selection and planning.

## Results

### Patient Positioning and Nasal Cavity Inspection

The specimens were placed in the simulated supine position in reverse Trendelenburg to approximately 15°. Subsequently, endoscopic inspection of the nasal cavities began.

### Nasoseptal Flap Harvesting

The right middle and superior turbinates were gently later-alized and the dissection proceeded along the middle and superior nasal corridors. The ostium of the sphenoid sinus was identified medial to the superior turbinate, 1.5 cm above the superolateral angle of the posterior choana (►Fig. 1A).

To harvest the nasoseptal flap, the superior incision started at the sphenoid ostium and ran parallel to the skull base approximately 1 cm inferior to the olfactory sulcus. When the incision reached the level of the anterior attachment of the middle turbinate, it was directed superiorly to incorporate the most anterosuperior area of the septal mucosa (►Fig. 1B). The inferior incision started at the superior margin of the choana and extended inferomedially to meet the nasal cavity floor (►Fig. 1C). The inferior incision continued anteriorly along the junction of the septum and nasal floor to the anterior margin of the septum. The incision progressed anteriorly along the nasal vault to the anterior edge of the septum (►Fig. 1D). Finally, the superior and inferior incisions were connected with a vertical incision at the mucocutaneous junction. The nasoseptal flap was elevated from the septal cartilage and bone in a subperichondrial/subperiosteal plane (►Fig. 1E). Preservation of the vascular pedicle was confirmed and the flap was stored in the nasopharynx (►Fig. 1F).<sup>18</sup>

### Endoscopic Endonasal Bilateral Complete Ethmoidectomy, Right Medial Maxillectomy, and Transethmoidal Sphenoidotomy

Bilateral anterior and posterior ethmoidectomies, transethmoidal sphenoidotomies, and right type A medial maxillectomy were modularly performed. After the right type A medial maxillectomy was completed, the nasoseptal flap was stored from the nasopharynx to the right maxillary sinus.

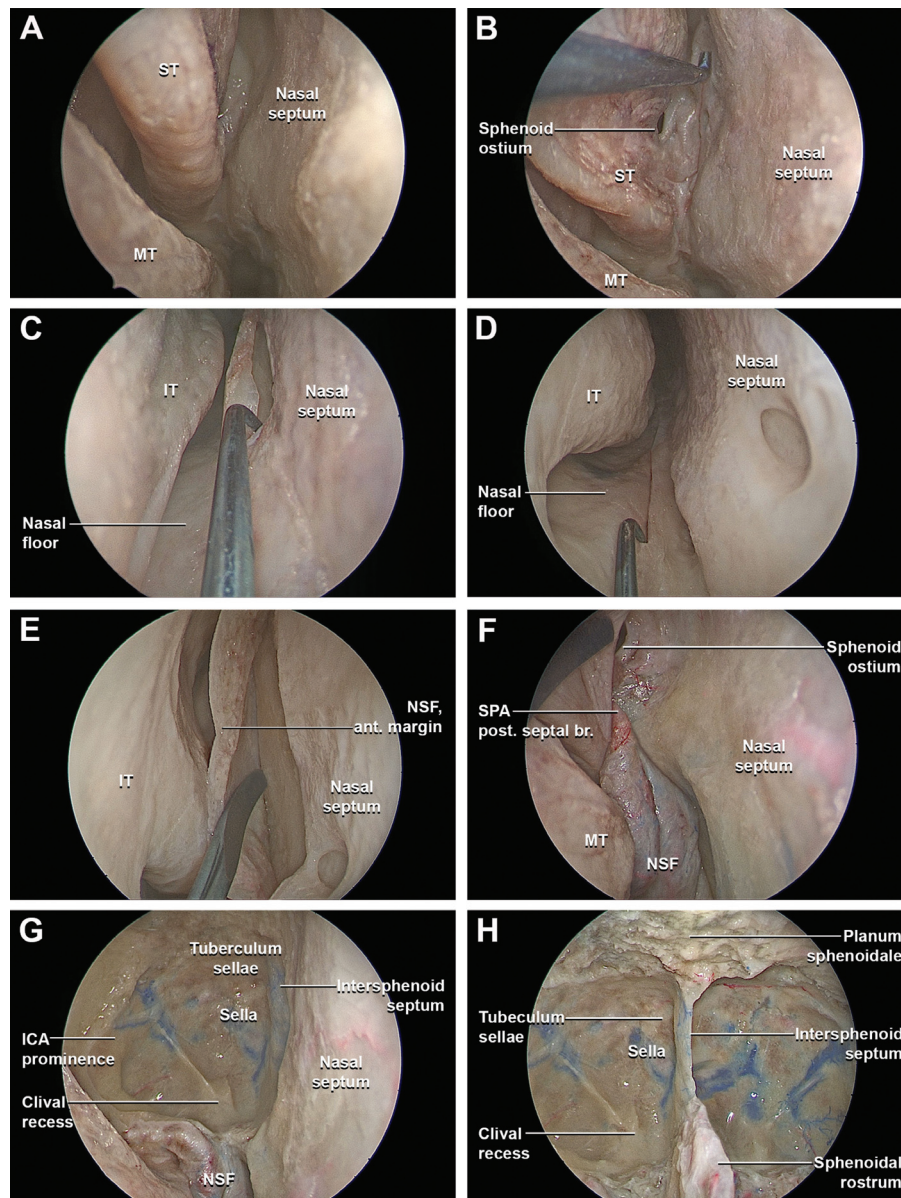


**Fig. 1** Stepwise dissection of the endoscopic endonasal nasoseptal flap harvesting, bilateral complete ethmoidectomy, and transtethmoidal sphenoidotomy. (A) The 0-degree endoscope is inserted in the nasal cavities along the middle nasal corridor. The middle nasal corridor is bounded by bulbous portion of the middle turbinate laterally and the nasal septum medially. The middle turbinate is gently lateralized, and, proceeding posteriorly through middle nasal corridor, the superior turbinate is identified and lateralized. The sphenothmoid recess is the space between the superior turbinate and the anterior wall of the sphenoid sinus, and its size varies according to the degree of pneumatization of the bulbous part of the superior turbinate. The sphenoid ostium is localized between the superior turbinate and the nasal septum. The posterior septal branch of the sphenopalatine artery is localized in the sphenothmoid recess. It travels from lateral to medial between the sphenoid ostium superiorly and choana inferiorly, ultimately vascularizing the nasal septum. (B) After all the landmarks have been identified, the nasoseptal flap is harvested. The posterior incision started 2 to 3 mm inferior to the sphenoid ostium in order to preserve the posterior septal artery. The incision then turns superiorly along the posterior margin of the nasal septum. The superior incision runs parallel to the skull base approximately 1 cm inferior to the nasal vault, at the level of the olfactory sulcus. (C) The inferior incision starts at the superior margin of the choana and extends medially along the posterior margin of the vomer toward the nasal floor. (D) The inferior incision continues anteriorly along the junction between the septum and nasal floor to the medial projection of the head of the inferior turbinate, at the level of the posterior boundary of the vestibular skin. (E) When the incision reaches the level of the anterior attachment of the middle turbinate, it is directed superiorly toward the nasal dorsum to incorporate the most anterior-superior area of the septal mucosa, connecting the superior and inferior incisions with a vertical incision at the mucocutaneous junction. The nasoseptal flap is elevated from the septal cartilage and bone in a subperichondrial and subperiosteal plane to the sphenoid rostrum and the anterior face of the sphenoid sinus with preservation of the vascular pedicle. (F) The nasoseptal flap is temporarily stored in the nasopharynx. (G) A bilateral anterior and posterior ethmoidectomy, transtethmoidal sphenoidotomy, and right medial maxillectomy are performed. (H) The intra-sphenoidal septations are carefully drilled flush with the floor of the sella, and the bony landmarks of the posterior wall of the sphenoid sinus are identified, including prechiasmatic sulcus, tuberculum recess, sellar prominence, clival recess, carotid prominences, and lateral optic-carotid recesses. ant., anterior; br., branch; ICA, internal carotid artery; IT, inferior turbinate; MT, middle turbinate; NSF, nasoseptal flap; post., posterior; SPA, sphenopalatine artery; ST, superior turbinate.

The intra-sphenoidal septations were drilled flush with the floor of the sella, and the bony landmarks of the posterior wall of the sphenoid sinus were identified. These included the optic prominences, prechiasmatic sulcus, tuberculum recess, sellar prominence, clival recess, carotid prominences, and lateral optic-carotid recesses (► Fig. 2A).

### Endoscopic Endonasal Midclivectomy and Partial Inferior Clivectomy with Nasopharyngeal Preservation

The rostrum sphenoidale was fractured and removed. Bilaterally, the inferior and medial portions of the vidian canals were progressively drilled out and followed posteriorly to identify the anterior limit of the foramen lacerum at the most posterior portion of the vidian canal (► Fig. 2B). Subsequently, the floor of the sphenoid sinus and the vaginal process of the sphenoid bone were drilled, exposing the medial aspect of the pterygosphenoidal fissure (i.e., synchondrosis between the lacerum process of the medial pterygoid plate and the floor of the sphenoid bone).<sup>19</sup> The lacerum process of the medial pterygoid plate, located inferomedial to the vidian canal, was drilled, identifying the lateral aspect of the pterygosphenoidal fissure and exposing the medial limit of the foramen lacerum. The fibrous tissue of the pterygosphenoidal fissure provides an excellent surgical landmark that can be followed during the endoscopic endonasal approach to foramen lacerum.<sup>19–22</sup> The vidian nerve was followed posteriorly within its canal until the lower portion of foramen lacerum was identified.<sup>19,21,23,24</sup> The pterygoid tubercle (i.e., triangular-shaped bony prominence located on the posterior surface of the medial pterygoid plate, medial to the vidian canal) was identified at the posterior convergence point between the pterygosphenoidal fissure and vidian canal.<sup>19,21</sup> The pterygoid tubercle was drilled, exposing the anterior limit of the foramen lacerum (► Fig. 2C).

The internal carotid artery (ICA) was skeletonized starting from the dura of the anterior wall of the cavernous sinus to its lacerum segment, thus maximizing mobilization of the paraclival ICA and providing access to the medial petrous apex located just posteriorly (► Fig. 2D).<sup>19</sup> After the paraclival ICAs were skeletonized bilaterally, the clival bone located immediately posterior and medial to the pterygosphenoidal fissure was removed laterally up to the petroclival fissure, exposing the ICA as it emerges from the carotid canal (► Fig. 2E).

Clival drilling proceeded inferiorly until visualization was obstructed by the floor of the sphenoid sinus. This exposure afforded better access to the medial petrous apex located just posterior to the paraclival ICA. To expose medial aspect of the lacerum ICA, clival bone immediately posterior and medial to the pterygosphenoidal fissure was completely removed. Just medial to the paraclival ICAs bilaterally, the abducens nerve was identified at the level of its proximal (and inferomedial) portion. While maintaining the integrity of the pharyngobasilar fascia with the muscles of the posterior nasopharynx, the superior portion of the lower clivus could be removed using a 70° angle drill and a 45° endoscope angled inferiorly (► Fig. 2F).

A linear, midline dural incision was made, and the anterior pontine membrane and underlying neurovascular structures within the prepontine cistern came into view (► Fig. 2G). The anterior prepontine membrane was removed, and the ventral brainstem and associated neurovascular structures were identified. Specifically, structures visualized included the upper third of the medulla, the ventral pons, the intradural segment of the vertebral arteries, basilar artery, pontine arteries, anterior inferior and posterior inferior cerebellar arteries, cisternal segments of the abducens nerves, and transverse pontine vein (► Fig. 2H–N).<sup>25</sup>

### Endoscopic Endonasal Complete Inferior Clivectomy and Partial-Superior Removal of the Anterior Arch of C1, and Partial-Superior Odontoidectomy (with Bilateral Incision of the Pterygosphenoidal Fissure Tissue and Anteroinferior Transposition of the Eustachian–Nasopharyngeal Complex)

The anatomy around the inferior portion of the foramen lacerum was better explored in order to identify relevant surgical landmarks. The foramen lacerum is filled in its inferior portion with fibrocartilaginous tissue that is strictly connected to the pharyngobasilar fascia inferomedially, the pterygosphenoidal fissure anteriorly, the petroclival fissure posteroinferiorly, and the petrosphenoidal fissure posterolaterally.<sup>19–21,23</sup> The Eustachian tube, traditionally divided into a proximal osseous and a distal cartilaginous portion, can be divided into five segments in an anterior-to-posterior direction according to an endoscopic endonasal surgically oriented classification, including the nasopharyngeal, pterygoid, lacerum, petrous, and bone segments.<sup>19–21,23</sup> The lacerum segment of the Eustachian tube runs just inferior to and attaches to the fibrocartilaginous portion of the foramen lacerum.<sup>19</sup> Then the Eustachian tube passes the scaphoid fossa (pterygoid segment), and continues anteromedially and inferiorly to the posterolateral wall of nasopharyngeal cavity (nasopharyngeal segment).<sup>19,21</sup>

The junction between the fibrocartilaginous tissues of the inferior foramen lacerum and the cartilage of the lacerum segment of the Eustachian tube was transected. The pterygosphenoidal fissure serves as a safe entry zone to the inferior foramen lacerum region. This sublacerum corridor along the inferior aspect of the petrous apex provides a safe surgical trajectory toward the ventral aspect of the petroclival fissure and jugular foramen, while mitigating the risk of carotid artery injury.<sup>19,22</sup>

The fibrocartilaginous tissues of foramen lacerum are also connected with the petroclival synchondrosis posterolaterally and the pharyngobasilar fascia anteromedially.<sup>19</sup> The disconnection of the fibrocartilaginous tissues of foramen lacerum from these two adhesions allows inferior transposition of the Eustachian tube and posterior nasopharynx (► Fig. 3A).<sup>26</sup>

The pharyngobasilar fascia and mucosa above torus tubarius were separated from the sphenoid sinus floor and medial pterygoid plate until the insertion of the pharyngobasilar fascia into the clival bone was reached (► Fig. 3B). Further dissection detached the nasopharyngeal and pterygoid segments of the Eustachian tube. Once the fibrocartilaginous adhesions of the Eustachian tube, petroclival synchondrosis,

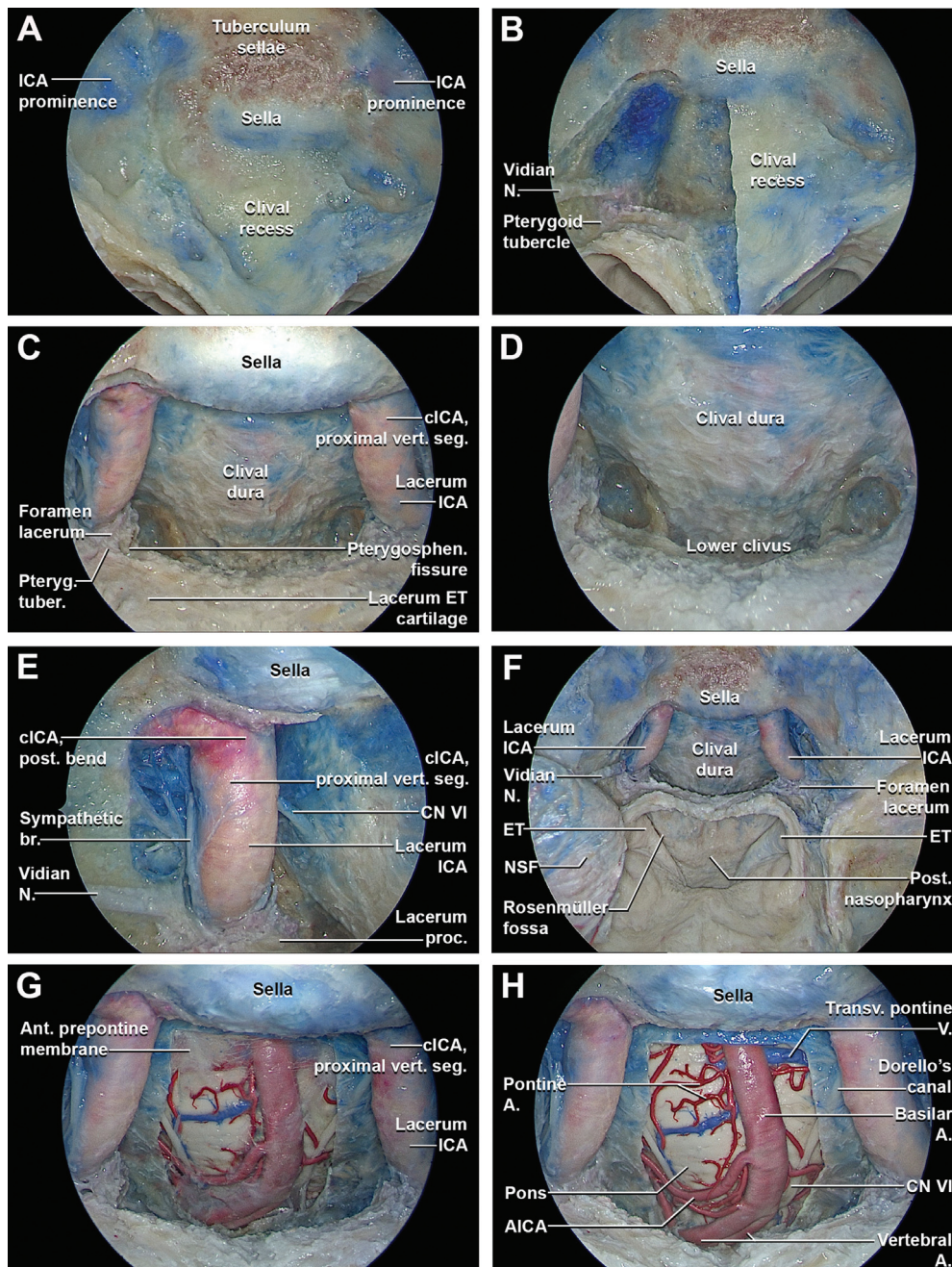


**Fig. 2** Stepwise dissection of the endoscopic endonasal midclivectomy and partial-superior inferior clivectomy (without nasopharyngeal incision or transposition of tissue). (A) After a complete extended transthemoidal sphenoidotomy the landmarks of the posterior walls of the sphenoid sinus are exposed, including the sella, clival recess, tuberculum sellae, and ICA prominences. (B) The right half of the midclivus is progressively drilled to the clival dura. The inferior and medial portions of the vidian canal are progressively removed in an anterior-to-posterior direction up to the level of the pterygoid tubercle. The vidian nerve runs anteriorly passing lateral to the lacerum ICA. The pterygoid tubercle is localized at the level of the anterior margin of the pterygosphenoidal fissure. (C) The midclivectomy is bilaterally performed up to the level of the paraclival ICA (i.e., lacerum ICA and proximal vertical segment of cavernous ICA). The bone covering the paraclival ICA is skeletonized. The pterygoid tubercle is removed, exposing the fibrocartilaginous tissue of the lower aspect of the foramen lacerum and the lacerum ICA just above it. (D) Using a 45° angle drill and an angle 45° optic directed downwards, the superior portion of the lower clivus is progressively drilled out, preserving the integrity of the pharyngobasilar fascia. (E) The anatomy around the paraclival ICA is explored. The distal portion of the vidian nerve serves as a landmark for the lacerum ICA, inferior to the lingual process, and inferomedial to V2. The sympathetic branch runs along the surface of the paraclival ICA and reaches at this level the abducens nerve. By drilling the lateral portion of the clival recess posteromedially to the lacerum ICA, the point where the abducens nerve pierces the dura and enters the Dorello's canal is identified bilaterally. The abducens nerve continues its course anteriorly, accessing the cavernous sinus through its posterior wall. (F) General view of the extended transthemoidal sphenoidotomy with endoscopic endonasal midclivectomy and partial-superior inferior clivectomy. The harvested NSF is stored in the right maxillary sinus. (G) The clival dura is opened, exposing the anterior preptentine membrane, lying between the clival dura and neurovascular structures of the brainstem. The anterior pontine membrane forms the anterior and lateral walls of the preptentine cistern and divides the preptentine cistern in medial and lateral preptentine cistern. (H) The anterior preptentine membrane is removed, exposing the ventral brainstem and its related vascular anatomy, including the ventral upper third of the medulla, the ventral pons, the intradural segment of the vertebral arteries, basilar artery, pontine arteries, cerebellar arteries, intracranial segment of abducens nerves, lateral anterior pontine vein, and transverse pontine vein. (Continued).

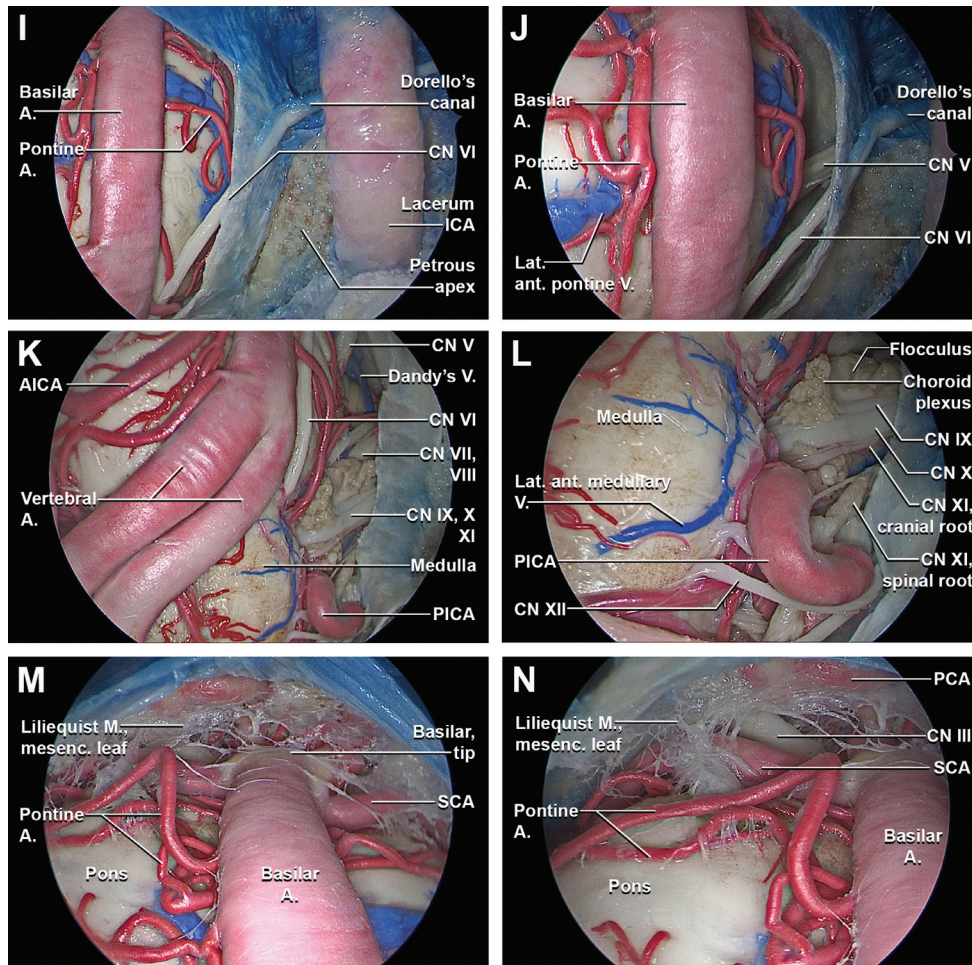


**Fig. 2** (I) Moving the 45° optic laterally the abducens nerve and the acoustic-facial bundle come into view. The abducens nerve emerges from the brainstem at the pontomedullary junction to enter the subarachnoid space, coursing upward between the pons and clivus to enter the Dorello's canal after piercing the clival dura. At the petrous apex, the abducens nerve angulates superolaterally to enter the posterior wall of the cavernous sinus, travelling in close proximity to the paraclival ICA. (J) The trigeminal nerve emerges at the ventrolateral surface of the pons, at the confluence of the cerebellar peduncles. (K) The foramen of Luschka and its choroid plexus, and the flocculus at the level of the lateral recess of the fourth ventricle have a consistent relationship with the facial and vestibulocochlear nerves. In most cases, the AICA passes below the facial and vestibulocochlear nerves as it encircles the brainstem, but it also may pass above or between these nerves in its course around the brainstem. The course of the superior petrosal vein may be above and lateral to the facial nerve, between the lateral limit of the trigeminal nerve and the medial limit of the facial nerve, or above and medial to the trigeminal nerve. After entering the vertebral canal, the extradural vertebral artery pierces the dura mater and courses intradurally superiorly over the anterolateral surface of the medulla oblongata. The intradural vertebral artery is placed between the hypoglossal nerve and the anterior root of the first cervical nerve and beneath the first digitation of the denticulate ligament. At the lower border of the pons, it unites with the contralateral vertebral artery to form the basilar artery. The basilar artery ascends along the ventral surface of the pons in its basilar groove within the pontine cistern. (L) A consistently identifiable tuft of choroid plexus hangs out of the foramen of Luschka and sits on the posterior surface of the glossopharyngeal and vagus nerves just inferior to the junction of the facial and vestibulocochlear nerves with the brainstem. The flocculus projects from the margin of the lateral recess of the fourth ventricle into the cerebellopontine angle, just posterior to where the facial and vestibulocochlear nerves join the pontomedullary sulcus. The PICA arises at the medullary level, encircles the medulla, passing in relationship to the glossopharyngeal, vagus, spinal accessory, and hypoglossal nerves to reach the surface of the inferior cerebellar peduncle. The glossopharyngeal, vagus, and spinal accessory nerves arise as rootlets that exit the brainstem and spinal cord along postolivary sulcus, a shallow groove between the olive and posterolateral surface of the medulla. The hypoglossal nerve arises as a line of rootlets that exit the brainstem along the anterior margin of the lower two-thirds of the olive in the preolivary sulcus, a groove between the olive and the medullary pyramid. The vertebral artery courses anterior to the lower cranial nerves. The hypoglossal rootlets usually pass behind the vertebral artery. (M) The upper margin of the durotomy is slightly retracted anteriorly and a 45° optic facing upwards is inserted to appreciate the upper limit of the pontine cistern. The SCA and the pontine arteries arise from the basilar artery and run horizontally on the ventral surface of the pons. The pontine cistern is separated from the interpeduncular cistern by the mesencephalic leaf of the Liliequist's membrane. The posterior free margin of the mesencephalic leaf may give some arachnoid trabeculae, which are extremely variable. The posterior communicating artery and its perforators together with the oculomotor nerve may pierce the membrane. (N) The oculomotor nerve runs above the superior cerebellar artery. The oculomotor nerve during its course is surrounded by an arachnoidal cuff that is an extension of the Liliequist's membrane until its entrance into the cavernous sinus, where it gives rise to the carotid-oculomotor membrane. The oculomotor nerve is not a site of attachment; it merely divides the mesencephalic leaf into a medial and a lateral part. The lateral attachment reaches the tentorium and forms the floor of the oculomotor cistern. The lateral pontomesencephalic membrane is the lateral extension of the mesencephalic leaf of the Liliequist's membrane.

A., artery; AICA, anterior inferior cerebellar artery; Ant., anterior; br., branch; cICA, cavernous segment of the internal carotid artery; CN, cranial nerve; ET, Eustachian tube; ICA, internal carotid artery; Lat., lateral; M., membrane; mesenc., mesencephalic; N., nerve; NSF, nasoseptal flap; post., posterior; proc., process; PICA, posterior inferior cerebellar artery; post., posterior; Pteryg., pterygoid; Pterygosphen., pterygosphenoidal; SCA, superior cerebellar artery; seg., segment; Transv., transverse; tuber., tubercle; V., vein; vert., vertical.

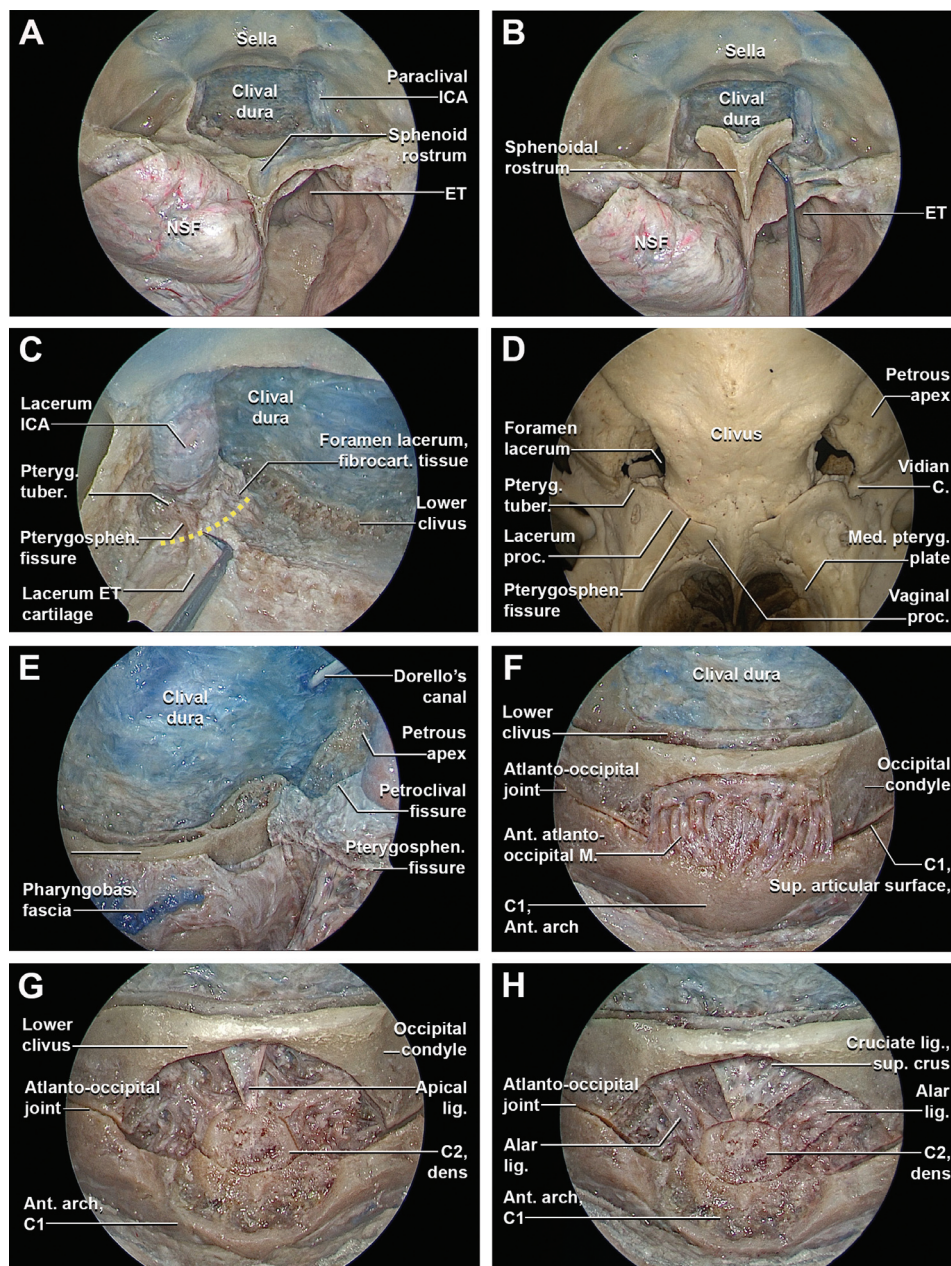


**Fig. 3** Stepwise dissection of the endoscopic endonasal complete inferior clivectomy, far-medial approach, partial-superior removal of the anterior arch of C1, and partial-superior odontoidectomy (with incision of the pterygosphenoidal fissure tissues). Endoscopic endonasal view with 0° optic (A–D) and with 30° optic (E–H). (A) The 0-degree endoscope is inserted in the nasal cavities and the clival dissection proceeds inferiorly. (B) The floor of the sphenoid sinus is removed, preserving the soft tissues of the posterior nasopharynx and the pharyngobasilar fascia. (C) The passage between the lacerum ICA and the proximal vertical segment of the cavernous ICA is completely exposed bilaterally by removing most inferior portion of the carotid prominences. At this level, the upper margin of the foramen lacerum is identified. The cartilaginous portion of the lacerum Eustachian tube is closely related to the pterygoid process, petrous apex, and foramen lacerum. The inferior portion of the foramen lacerum is filled with fibrocartilaginous tissue that features dense connections to the pharyngobasilar fascia inferomedially, the pterygosphenoidal fissure anteriorly, the petroclival fissure inferoposteriorly, and the petrosphenoidal fissure posterolaterally. This soft tissue provides reliable landmark for localization of the inferior aspect of the foramen lacerum during EEAs. Just anteromedially to the passage through the lacerum foramen of the sympathetic branch, the cartilage of the lacerum Eustachian tube enters into close relationship and attaches to the fibrocartilaginous tissue of the foramen lacerum. (D) Osseous anatomy of the foramen lacerum as seen from a posteroinferior view. On the posterior surface of the pterygoid process, the pterygoid tubercle is a triangular-shaped area located between the vidian canal and the pterygosphenoidal fissure that forms the anterior wall of the lower part of foramen lacerum. (E) The inferior wall of the foramen lacerum is progressively exposed bilaterally through a sublacerum corridor transecting the pterygosphenoidal fissure tissues and detaching the cartilage of the lacerum Eustachian tube from the inferior foramen lacerum. The inferior portion of the lower clivus and the atlanto-occipital joints are exposed. (F) By detaching the pharyngobasilar fascia, the anterior atlanto-occipital membrane is exposed. The anterior atlanto-occipital membrane is broad and composed of densely woven fibers, which pass between the anterior margin of the foramen magnum above, and the upper border of the anterior arch of the atlas below. Laterally, it is continuous with the articular capsules. (G) The anterior atlanto-occipital membrane is removed exposing the anterior arch of C1. The superior portion of the anterior arch of C1 is drilled out exposing the tip of the dens of C2 and the apical ligament. The apical ligament is a small ligament that joins the tip of the dens of C2 to the anterior margin (basion) of the foramen magnum. (H) By detaching the apical ligament and the bilateral alar ligaments and the superior crus of the cruciate ligament are exposed. (*Continued*).

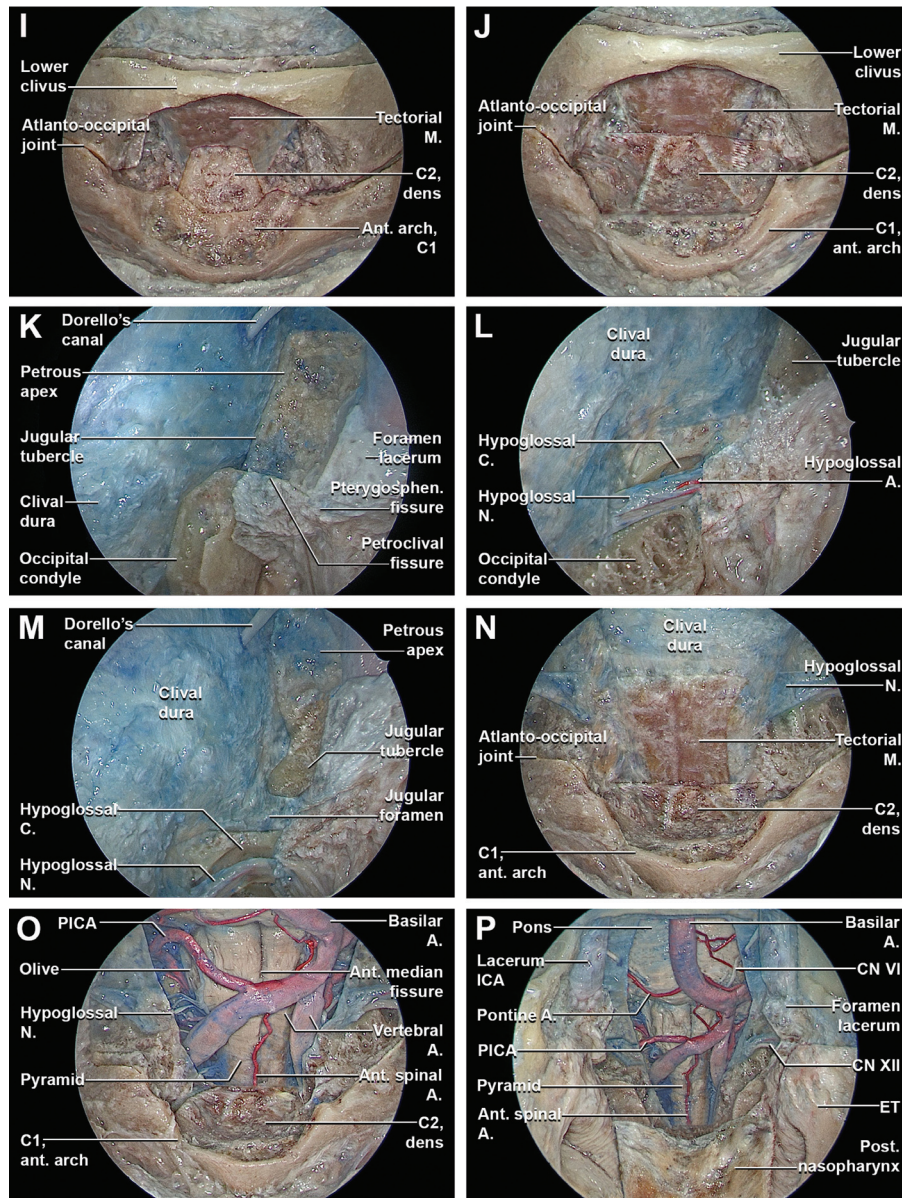


**Fig. 3** (I) The bilateral alar ligaments and the superior crus of the cruciate ligament are removed, better exposing the tip of the dens of C2. (J) A selective superior odontoidectomy is performed and in a more posterior coronal plane the tectorial membrane is exposed. The tectorial membrane is a superior continuation of the posterior longitudinal ligament, connecting the dorsal aspect of the dens and the vertebral bodies of C2 and C3 to the clivus, attaching along the anterior margin of the foramen magnum. Along with the alar ligament, it prevents anterior subluxation of the head on the cervical spine and limits flexion. (K) The inferior clivectomy is completed. Subsequently, with a 45° optic, the dissection proceeds at the level of the inferolateral clival region completing the far-medial approach. Just superior to the inferolateral clival region, the Gardner's triangle is identified, bounded superiorly by the abducens nerve, anteriorly by the paraclival ICA, and inferiorly by the petroclival synchondrosis. This triangle provides access to the petrous apex. (L) Transcondylar part of the far-medial approach. The capsule of the atlanto-occipital joint is removed, exposing the supracondylar groove. The supracondylar groove provides insertion for the rectus capitis anterior muscle, anterior atlanto-occipital membrane, and capsule joint. This supracondylar groove is a reliable landmark for estimating the position of the hypoglossal canal, which are situated just posterior and lateral to the groove, respectively (M) Transtuberular part of the far-medial approach. (N) The superior attachment of the tectorial membrane is detached and the tectorial membrane is progressively transposed inferiorly, exposing the underlying clival and upper cervical spine dura. (O) The dura is longitudinally incised exposing the proximal portion of intradural vertebral artery and the first cervical nerve. The anterior spinal artery originates from two smaller vessels from each vertebral artery which unite at the level of the upper portion of the medulla oblongata. The anterior spinal artery then passes through the foramen magnum and descends along the anterior aspect of the spinal cord, running at the level of the anterior median fissure and supplying the anterior portion of the spinal cord. The rootlets that form the hypoglossal nerve arise from the medulla in the preolivary sulcus and travel anterolaterally through the subarachnoid space, passing behind the vertebral artery to reach the hypoglossal canal. (P) General overview of the endoscopic endonasal middle and inferior clivectomy, with partial-superior removal of the anterior arch of C1, partial-superior odontoidectomy, and bilateral far medial approach after bilateral incision of the pterygosphenoidal fissure tissue and anteroinferior transposition of the Eustachian–nasopharynx complex. A., artery; ant., anterior; C., canal; CN, cranial nerve; ET, Eustachian tube; fibrocart., fibrocartilaginous; ICA, internal carotid artery; lig., ligament; M., membrane; Med., medial; N., nerve; NSF, nasoseptal flap; PICA, posterior inferior cerebellar artery; Pharyngobas., pharyngobasilar; proc., process; Pteryg., pterygoid; Pterygosphen., pterygosphenoidal; sup., superior; tuber., tubercle.

This document was downloaded for personal use only. Unauthorized distribution is strictly prohibited.



and pharyngobasilar fascia were completely disconnected from the inferior portion of the foramen lacerum, the Eustachian–nasopharyngeal complex (i.e., Eustachian tube, prevertebral fascia, and longus capitis and rectus capitis muscles) was transposed inferiorly, better exposing the lower clivus and craniocervical junction (►Fig. 3C, D).

The superior and inferior attachments of the anterior atlanto-occipital membrane were exposed and dissected from the bone, identifying the anterior arch of C1 and the bilateral atlanto-occipital joints (►Fig. 3E, F). The inferior portion of the lower clivus and the superior portion of the anterior arch of C1 were drilled, exposing the tip of the odontoid process and apical ligament. The apical ligament was identified anterior to the alar and cruciate ligaments (►Fig. 3G). By transecting the apical ligament and the bilateral alar ligaments, the superior crus of the cruciate ligament was identified and removed, providing visualization of the tectorial membrane (►Fig. 3H, I). The superior portion of the odontoid process was then drilled (►Fig. 3J). The superior attachment of the tectorial membrane was detached and transposed inferiorly, exposing the underlying clival and upper cervical dura. The dural incision was extended inferiorly, better exposing the proximal portion of the intradural vertebral arteries and the C1 nerve root.

#### Far-Medial Extension

Once the standard inferior clivectomy was completed, lateral extensions of the clivectomies were performed. To access the hypoglossal canal, the supracondylar groove was exposed deep to the atlanto-occipital joint capsule and was progressively drilled until exposure of the hypoglossal canal and its dural covering was afforded (►Fig. 3K, L). To increase the lateral exposure towards the jugular foramen, the jugular tubercle was drilled laterally until the medial edge of the jugular foramen. This provided access to cranial nerves IX, X, and XI at their distal intracranial course (►Fig. 3M–P).

#### Endoscopic Endonasal Complete Removal of the Anterior Arch of the Atlas and Odontoidectomy (with Bilateral Para-Eustachian Incision of the Posterior Wall of Nasopharynx)

The mucosal and muscular layers of the posterior nasopharynx and the pharyngobasilar fascia were incised just medial to the torus tubarius of the Eustachian tube bilaterally, and transposed inferiorly (►Fig. 4A). Longus capitis, rectus capitis anterior, and anterior longitudinal ligament were exposed and inferiorly displaced to provide better access to the entirety of the anterior arch of C1, the atlantoaxial joint, and the anterior surface of the body of C2 (►Fig. 4B, C). Bilateral osteotomies were performed at the lateral extents of the anterior arch of C1 and it was removed en-bloc (►Fig. 4D). The base of the odontoid process was drilled and the odontoid process was removed, exposing the underlying cruciate ligament (►Fig. 4E). The cruciate ligament and the tectorial membrane were incised and dissected exposing the upper cervical dura (►Fig. 4F, G). The previous dural incision was extended inferiorly, better exposing the neurovascular anatomy of the upper cervical spinal cord, including the ventral C2 nerve root, spinal roots of the accessory nerve,

and the distal portion of the extradural vertebral artery within sulcus arteriosus (►Fig. 4H).

## Representative Case Review

### Case 1: Clival Chordoma Surgically Treated with Endoscopic Endonasal Midclivectomy and Partial-Inferior Clivectomy with Nasopharyngeal Preservation

A neurologically intact 31-year-old female with a history of headache underwent a brain magnetic resonance imaging (MRI) that revealed a clival lesion involving the middle and upper portion of the lower clivus, with intradural extension into the posterior cranial fossa. Mass effect on the ventral pons was present (►Fig. 5A, B). An endoscopic endonasal midclivectomy and partial inferior clivectomy with nasopharyngeal preservation was utilized. Reconstruction was performed with collagen graft and right-sided nasoseptal flap. Gross total resection of the lesion was achieved (►Fig. 5C). Histopathological examination confirmed the diagnosis of chordoma. The postoperative course was uneventful and the patient was discharged home on postoperative day 5. No adjuvant radiotherapy was given and the patient remains without evidence of disease 12 months after resection.

### Case 2: Clival Chordoma Surgically Treated with Endoscopic Endonasal Midclivectomy and Partial-Inferior Clivectomy with Bilateral Para-Eustachian Nasopharyngeal Incision

A 52-year-old female with a history of episodes of blurred and double vision associated with headaches and nausea presented to our clinic for worsening symptoms. MRI showed a large intracranial clival lesion with bone erosion and intradural extension, involving the middle and lower clivus, sellar floor, and, bilaterally, the ventral jugular tubercle and occipital condyle (►Fig. 5D, E). The patient initially underwent a C0–C2 fusion to prevent instability of the craniocervical junction (CCJ) followed 2 weeks later by an endonasal midclivectomy, partial inferior clivectomy, and bilateral far-medial extension, with para-Eustachian nasopharyngeal incisions for tumor resection. An aggressive subtotal resection was performed and reconstruction was performed with collagen graft and fat graft. The patient was neurologically stable after surgery. Histopathological examination confirmed the diagnosis of chordoma. She then received proton beam therapy to a total dose of 70 Gy and remains free from tumor progression 12 months following completion of therapy.

### Case 3: Odontoid Process Fracture—Endoscopic Endonasal Odontoidectomy (with Bilateral Para-Eustachian Incision of the Posterior Wall of Nasopharynx)

A 53-year-old female with a history of Goldenhar syndrome presented to our clinic with worsening clumsiness in her right hand and sensory disturbances in all four extremities. MRI indicated posterior displacement of her C1–C2 vertebrae causing severe cervical stenosis and cranial settling. Given the progression of her symptoms, and multiple previous

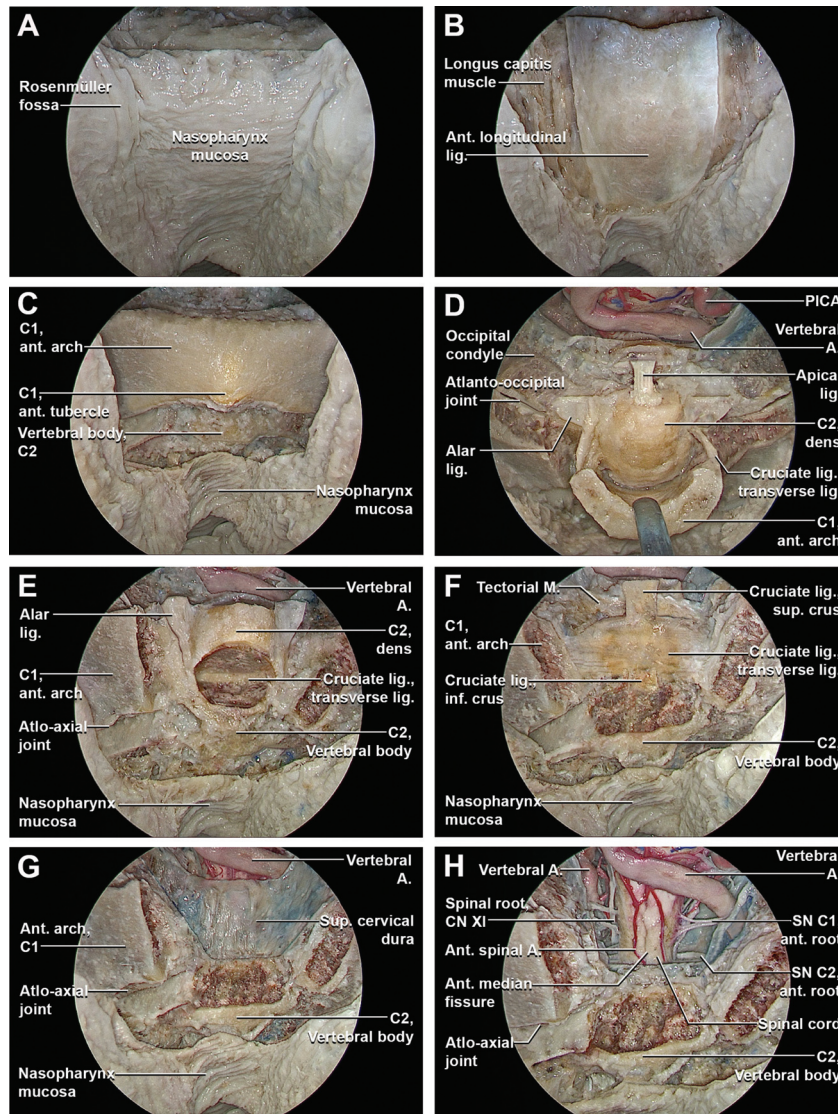


**Fig. 4** Stepwise dissection of the endoscopic endonasal complete removal of the anterior arch of the atlas and odontoidectomy (with incision of the posterior wall of nasopharynx). (A) Using a 45° optic facing downwards, the dissection moves inferiorly at the level of the posterior nasopharynx. (B) The mucosal and muscular layer of the posterior wall of the nasopharynx and the basopharyngeal fascia are incised bilaterally, just medial to the Eustachian tube. (C) The longus capitis and rectus capitis anterior with the anterior longitudinal ligament are transposed inferiorly providing access to the entirety of the anterior arch of C1, the atlantoaxial joint, and the anterior surface of the body of C2. (D) The anterior arch of C1 is drilled bilaterally. The insertions of the transverse ligament at the level of the posterior surface of the anterior arch of C1 are transected and the anterior arch of C1 is removed en-bloc, showing the odontoid process with its ligaments attached. (E) The base of the dens of C2 is drilled and the odontoid process, with the alar ligaments and the apical ligament previously disconnected from the anterior margin of the foramen magnum, are removed, exposing the underlying cruciate ligament. (F) The cruciate ligament of the atlas consists of the transverse ligament of the atlas and the longitudinal band, divided in superior longitudinal band (superior crus), and an inferior longitudinal band (inferior crus). The longitudinal band lying between the apical ligament and tectorial membrane. The superior longitudinal band connects the transverse ligament to the anterior side of the foramen magnum, while the inferior longitudinal band connects the transverse ligament to the body of the axis. The longitudinal bands prevent hyperflexion and hyperextension of the occipital bone, and hold the transverse ligament of the atlas in a normal position. The transverse ligament attaches to a small tubercle on the medial cortex of the atlas lateral masses on both sides, anterior to the tectorial membrane and dura. It passes posterior to the dens, with a small intervening synovial capsule, fixing the dens to the posterior margin of the anterior arch of the atlas and stabilizing the atlanto-odontoid joint. (G) The cruciate ligament with the inferior portion of the tectorial membrane are incised and removed and the superior cervical dura is exposed. (H) The exposed cervical dura is incised exposing the neurovascular anatomy of the upper cervical spinal cord, including the first and second cervical nerves, the spinal root of the accessory nerve, and the distal portion of the extradural vertebral artery within the vertebral canal. The first cervical nerve originates at the level of the passage between the medulla oblongata and the cervical spinal cord and it pierces the dura just inferior to the extra- to intradural passage of the vertebral artery. The first cervical nerve carries predominantly motor fibers, but also a small meningeal branch that supplies sensation to parts of the dura around the foramen magnum lacks a ganglion. Unlike the other cervical spinal nerves, the first cervical nerve lacks of a ganglion. The sensory and motor root of the second cervical nerve are identified just below to first cervical nerve. The second cervical nerve ganglion lies on posterior surface of the atlantoaxial articulation in correspondence of the intervertebral space, which is bordered superiorly by the posterior arch of atlas, inferiorly by the lamina of axis, anteriorly by the lateral atlantoaxial joint and its fibrous capsule, and posteriorly by the anterior edge of the ligamentum flavum. The spinal root of the accessory nerve (XI) arises from motor roots of C1–C6 and unite to form a single trunk. Then, the spinal root of CN XI enters the skull through foramen magnum, and is then directed to the jugular foramen where it exits the intradural space. A., artery; ant., anterior; CN, cranial nerve; inf., inferior; lig., ligament; M., membrane; PICA, posterior inferior cerebellar artery; SN, spinal nerve; sup, superior.

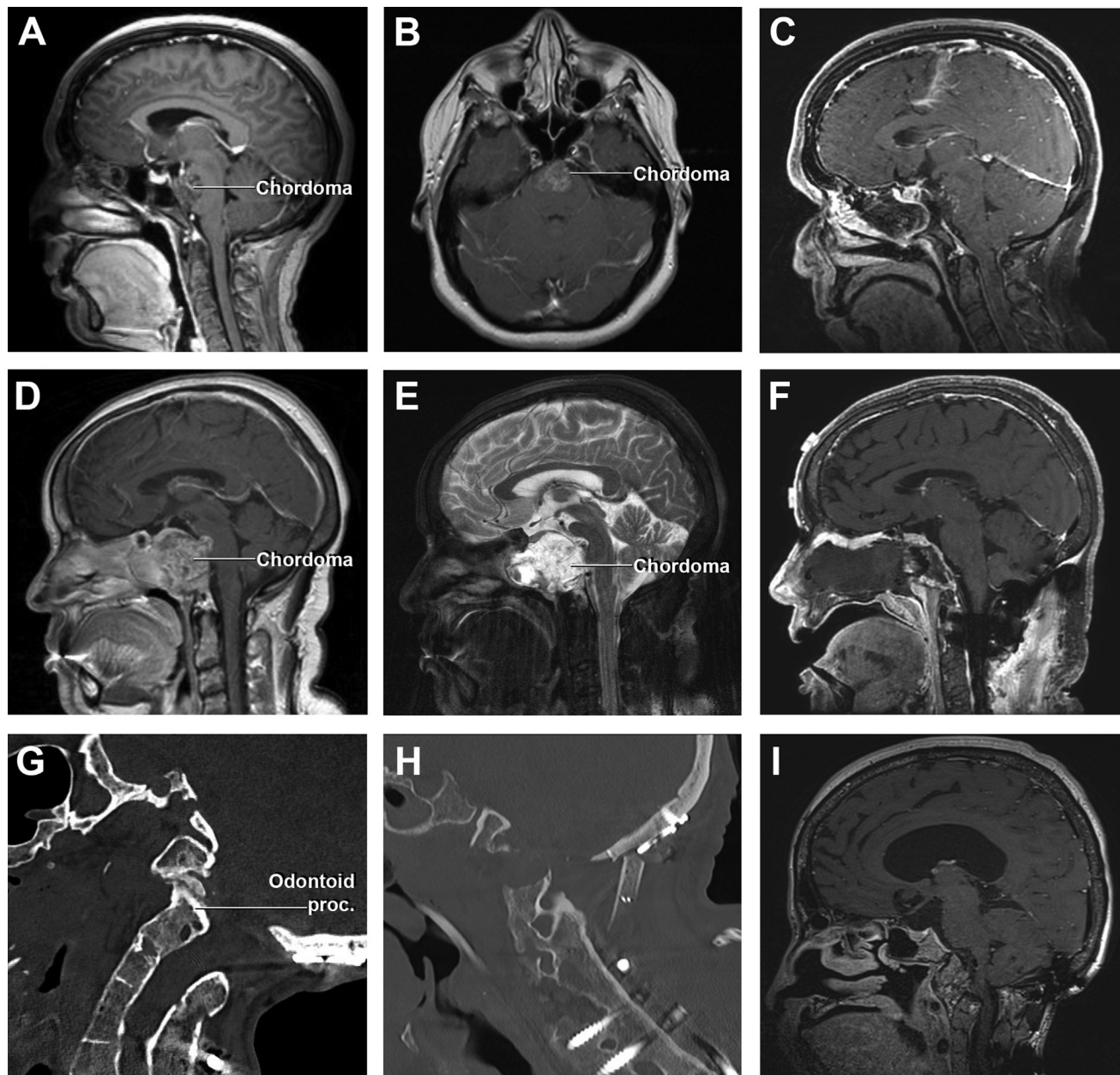


**Fig. 5** Illustrative cases. (A and B: case 1) Preoperative contrast-enhanced T1-weighted sagittal and coronal MRIs demonstrate a large, heterogeneously enhancing clival lesion involving the middle and upper portion of the lower clivus, with intradural extension into the posterior fossa. (C: case 1) Postoperative contrast-enhanced T1-weighted sagittal MRI confirms gross total resection of the lesion. (D and E: case 2) Preoperative T1 and T2-weighted sagittal MRI shows a large intracranial clival lesion with bone erosion and extradural extension, involving the middle and lower clivus, sellar floor, and bilateral extension to the ventral jugular tubercle and occipital condyle. (F: case 2) Postoperative contrast-enhanced T1-weighted sagittal MRI in the sagittal plane shows subtotal resection of the lesion, with a small nodule of residual tumor abutting the ventral pons and residual tumor in the left occipital condyle gross total resection of the injury. (G: case 3) Preoperative CT shows a fracture of the odontoid process. (H and I case 3) Postoperative CT and contrast-enhanced T1-weighted sagittal MRI in the plane show successful decompression of the CCJ. CT, contrast enhanced; MRI, magnetic resonance imaging.

cervical surgeries, decompression of her CCJ was offered through an endoscopic endonasal inferior clivectomy and odontoidectomy. The patient was discharged home on POD 12 with no new neurological deficits.

## Discussion

In this study we described the basic steps, anatomy, and nuances of the endoscopic endonasal middle and inferior

clivectomies, far-medial approach, and odontoidectomy. We previously described the technique for anteroinferior transposition of the Eustachian–nasopharynx complex after transecting the soft tissues of the pterygosphenoidal fissure and disconnecting the fibrocartilaginous borders of the Eustachian tube with preservation of the nasopharyngeal mucosa.<sup>19,22</sup> Through the EETCAs, unobstructed access to neurovascular anatomy of the ventral brainstem was afforded.

Given the many neurovasculature structures that surround or are involved in the EETCAs, identification of landmarks that facilitate safe dissection is paramount. First, proper localization of foramen lacerum is crucial to minimize the risk of ICA injury. The vidian canal is the most useful landmark for the lacerum ICA from the endoscopic endonasal trajectory.<sup>19,24</sup> The vidian canal is located at the lateral aspect of the floor of the sphenoid sinus within the body of the pterygoid, and, once identified, can be carefully followed posteriorly to find the lacerum ICA as it turns vertically just medial to the vidian canal and its contents. The vidian canal converges posteriorly with the pterygosphenoidal fissure, and as drilling progresses in between them, the pterygoid tubercle will remain between the pterygosphenoidal fissure and the vidian canal to form the anterior inferior part of the foramen lacerum.<sup>19</sup>

Several lesions of the posterior fossa may be amenable to EETCAs, including tumors, vascular malformations, and craniocervical junction abnormalities.<sup>27,28</sup> Benefits of the EETCA to lesions of the posterior fossa include a working corridor mostly medial to involved neurovasculature, adequate illumination and magnification of the operative field, and potentially early devascularization of the lesions' blood supply in case of meningiomas.<sup>27</sup> EETCAs are now commonly utilized for most chordomas of the clivus as the tumor's usually soft consistency facilitates its dissection away from involved neurovasculature.<sup>5,8,29–42</sup> Despite growing experience with these approaches, utilization of the EETCAs for other posterior fossa lesions—including meningiomas and vascular lesions—remains controversial.<sup>43,44</sup> For clival tumors, hesitancy in utilizing this approach may be the inability to perform bimanual dissection—especially when the lesion is suspected to be adherent to surrounding structures. For vascular lesions, difficulty in attaining control for aneurysms and controlling inadvertent bleeding for other malformations may obviate the use of the EETCAs. Despite these limitations, several publications have described this approach for petroclival/clival meningiomas,<sup>43,44</sup> aneurysms,<sup>27,45,46</sup> and cavernous malformations.<sup>31,47–52</sup> Approach selection for lesions that have anatomical equipoise should be guided by a surgeon's comfort with the different approaches. Endoscopic endonasal approaches have also been effective for treating craniocervical junction abnormalities. Indications for this approach have included severe basilar invagination, displaced os odontoideum, pannus with mass effect, and retroflexed odontoid processes associated with Chiari malformation Type 1.<sup>27,53</sup> With respect to open strategies for addressing these pathologies, however, the endoscopic endonasal approaches may be more invasive and offer more constrained corridors with limited surgical maneuverability.

Lateral extension of the corridor is often limited for most endoscopic endonasal approaches. For the EETCAs, lateral extension is limited by the paraclival ICA, Eustachian tube, and jugular foramen.<sup>14,54</sup> If a lesion extends lateral to these structures and an EETCA is still indicated, lateral exposure can be supplemented with technology including angled endoscopes and instruments, transposition of the Eustachian

tube, and drilling of the jugular tubercle.<sup>14,54–57</sup> Despite being able to expose these lateral structures in a cadaveric setting, copious venous bleeding from the basilar venous plexus during bone removal can limit the lateral access of these approaches and, of course, careful hemostasis of any venous bleeding should be performed before continuing with the intradural portion of the dissection.<sup>55</sup>

Inferior extension can be supplemented by detachment and anteroinferior transposition of the Eustachian–nasopharynx complex. Without any manipulation of the posterior nasopharynx, the inferior limit is approximately at the level of the lower clivus. If the Eustachian–nasopharynx complex is mobilized anteroinferiorly through bilateral pterygosphenoidal fissure tissue transection (→**Fig. 3C**) but without incision of the posterior nasopharynx, the inferior limit of the EETCA is the upper craniocervical junction. To maximize the inferior reach of the EETCA, sharply dividing the posterior nasopharynx affords access to the C2 nerve roots.<sup>53</sup>

Complications of the EETCAs are mainly due to the risk of injuring the paraclival ICAs, the basilar artery and its pontine perforators, and the abducens nerve in the prepontine cistern as it enters Dorello's canal.<sup>9,27,28,42</sup> The risk of injury to the paraclival ICAs can increase if the bone covering the ICA is removed to improve the surgical access laterally.<sup>58</sup> In order to reduce the risk of injury to the intracranial vessels, careful study of preoperative imaging and intraoperative Doppler ultrasound may help identify the precise location of the underlying vasculature prior to opening the dura.<sup>27</sup> Another drawback of the EETCAs is the increased risk of CSF leak.<sup>28,59</sup> To mitigate the risk of postoperative CSF leak, robust multilayered skull base reconstruction is required. For posterior fossa defects, reconstruction often includes autologous fat, fascia lata, and a pedicled nasoseptal flap.<sup>27,28,60–63</sup> We hypothesize that preserving the nasopharyngeal mucosa may decrease the risk of postoperative CSF leak.<sup>22</sup> Additionally, postoperative lumbar drainage has been shown to significantly decrease the risk of postoperative CSF leak for large posterior fossa defects.<sup>61–63</sup> Despite the advancement of techniques and the growing experience of skull base surgeons, CSF leak remains a significant issue with reported rates of 16.5% for EETCAs with multilayer reconstruction.<sup>27</sup>

## Conclusion

Mastery of the surgical steps and anatomical landmarks of the endoscopic endonasal middle and inferior clivectomies, far-medial approach, and odontoidectomy is required prior to their utilization in a clinical setting. Thus, we provide a succinct, yet comprehensive, description of the main steps and technical nuances of the EETCAs for trainees in skull base surgery.

### Ethical Approval

This retrospective chart review study involving human participants was in accordance with the ethical standards of the institutional and national research committee and

with the 1964 Helsinki Declaration and its later amendments or comparable ethical standards. The Human Investigation Committee (IRB) of the Mayo Clinic approved this study.

#### Funding

This work was supported in part by Joseph I. and Barbara Ashkins Endowed Professorship in Neurosurgery and by Charles B. and Ann L. Johnson Endowed Professorship in Neurosurgery.

#### Conflict of Interest

None declared.

#### Acknowledgments

We thank the Fondazione Beretta for their constant devotion to supporting brain cancer research.

#### References

- Kim YH, Jeon C, Se Y-B, et al. Clinical outcomes of an endoscopic transclival and transpetrosal approach for primary skull base malignancies involving the clivus. *J Neurosurg* 2018;128(05):1454–1462
- Shkarubo AN, Koval' KV, Dobrovol'skiy GF, et al. Extended endoscopic endonasal posterior (transclival) approach to tumors of the clival region and ventral posterior cranial fossa. Part 1. Topographic and anatomical features of the clivus and adjacent structures [in Russian]. *Vopr Neurokhir* 2017;81(04):5–16
- Rhoton AL Jr. The cerebellopontine angle and posterior fossa cranial nerves by the retrosigmoid approach. *Neurosurgery* 2000;47(03):S93–S129
- Al-Mefty O, Kadri PAS, Hasan DM, Isolan GR, Pravdenkova S. Anterior clivectomy: surgical technique and clinical applications. *J Neurosurg* 2008;109(05):783–793
- Fernandez-Miranda JC, Gardner PA, Snyderman CH, et al. Clival chordomas: a pathological, surgical, and radiotherapeutic review. *Head Neck* 2014;36(06):892–906
- Kassam AB, Gardner P, Snyderman C, Mintz A, Carrau R. Expanded endonasal approach: fully endoscopic, completely transnasal approach to the middle third of the clivus, petrous bone, middle cranial fossa, and infratemporal fossa. *Neurosurg Focus* 2005;19(01):E6
- Bossi Todeschini A, Montaser AS, Hardesty DA, Carrau RL, Prevedello DM. The limits of the endoscopic endonasal transclival approach for posterior fossa tumors. *J Neurosurg Sci* 2018;62(03):322–331
- Frank G, Sciarretta V, Calbucci F, Farneti G, Mazzatenta D, Pasquini E. The endoscopic transnasal transsphenoidal approach for the treatment of cranial base chordomas and chondrosarcomas. *Neurosurgery* 2006;59(1, Suppl 1):ONS50–ONS57, discussion ONS50–ONS57
- Shkarubo AN, Koval' KV, Dobrovol'skiy GF, et al. Extended endoscopic endonasal posterior (transclival) approach to tumors of the clival region and ventral posterior cranial fossa. Part 2. Topographic and anatomical aspects and surgical technique [in Russian]. *Vopr Neurokhir* 2017;81(05):17–30
- Shkarubo AN, Koval' KV, Shkarubo MA, Chernov IV, Andreev DN, Panteleyev AA. Endoscopic endonasal transclival approach to tumors of the clivus and anterior region of the posterior cranial fossa: an anatomic study. *World Neurosurg* 2018;119:e825–e841
- Shkarubo AN, Koval' KV, Chernov IV, Andreev DN, Kurnosov AB, Panteleyev AA. Endoscopic endonasal transclival removal of tumors of the clivus and anterior region of the posterior cranial fossa (results of surgical treatment of 140 patients). *Chin Neurosurg J* 2018;4:36
- Oostra A, van Furth W, Georgalas C. Extended endoscopic endonasal skull base surgery: from the sella to the anterior and posterior cranial fossa. *ANZ J Surg* 2012;82(03):122–130
- Messina A, Bruno MC, Decq P, et al. Pure endoscopic endonasal odontoidectomy: anatomical study. *Neurosurg Rev* 2007;30(03):189–194, discussion 194
- Simal-Julián JA, Miranda-Lloret P, Beltrán-Giner A, Plaza-Ramirez E, Botella-Asunción C. Full endoscopic endonasal extreme far-medial approach: Eustachian tube transposition. *J Neurosurg Pediatr* 2013;11(05):584–590
- Zoli M, Mazzatenta D, Valluzzi A, Mascari C, Pasquini E, Frank G. Endoscopic endonasal odontoidectomy. *Neurosurg Clin N Am* 2015;26(03):427–436
- Komune N, Matsuo S, Miki K, et al. Surgical anatomy of the eustachian tube for endoscopic transnasal skull base surgery: a cadaveric and radiologic study. *World Neurosurg* 2018;112:e172–e181
- Leonel LCP, Carlstrom LP, Graffeo CS, et al. Foundations of advanced neuroanatomy: technical guidelines for specimen preparation, dissection, and 3D-photodocumentation in a surgical anatomy laboratory. *J Neurol Surg B Skull Base* 2021;82(Suppl 3):e248–e258
- Pinheiro-Neto CD, Snyderman CH. Nasoseptal flap. *Adv Otorhinolaryngol* 2013;74:42–55
- Wang WH, Lieber S, Mathias RN, et al. The foramen lacerum: surgical anatomy and relevance for endoscopic endonasal approaches. *J Neurosurg* 2018;1:1–12
- Ozturk K, Snyderman CH, Gardner PA, Fernandez-Miranda JC. The anatomical relationship between the eustachian tube and petrous internal carotid artery. *Laryngoscope* 2012;122(12):2658–2662
- Liu J, Pinheiro-Neto CD, Fernandez-Miranda JC, et al. Eustachian tube and internal carotid artery in skull base surgery: an anatomical study. *Laryngoscope* 2014;124(12):2655–2664
- Pinheiro-Neto CD, Salgado-Lopez L, Leonel LCPC, Aydin SO, Peris-Celda M. Endoscopic endonasal approaches to the clivus with no violation of the nasopharynx: surgical anatomy and clinical illustration. *J Neurol Surg B Skull Base* 2021;83(Suppl 2):e374–e379
- Keshelava G, Mikadze I, Abzianidze G, Kikalishvili L, Kakabadze Z. Surgical anatomy of petrous part of the internal carotid artery. *Neuroanat* 2000;8:46–48
- Pinheiro-Neto CD, Fernandez-Miranda JC, Rivera-Serrano CM, et al. Endoscopic anatomy of the palatovaginal canal (palatosphenoidal canal): a landmark for dissection of the vidian nerve during endonasal transpterygoid approaches. *Laryngoscope* 2012;122(01):6–12
- Matsuno H, Rhoton AL Jr, Peace D. Microsurgical anatomy of the posterior fossa cisterns. *Neurosurgery* 1988;23(01):58–80
- McDavid LJ, Khan YS. *Anatomy, Head and Neck, Prevertebral Muscles*. Treasure Island, FL: StatPearls Publishing; 2022
- Belotti F, Tengattini F, Mattavelli D, et al. Transclival approaches for intradural pathologies: historical overview and present scenario. *Neurosurg Rev* 2021;44(01):279–287
- Little RE, Taylor RJ, Miller JD, et al. Endoscopic endonasal transclival approaches: case series and outcomes for different clival regions. *J Neurol Surg B Skull Base* 2014;75(04):247–254
- Zenonos G, Alkhalili K, Koutourousiou M, et al. Endoscopic endonasal approach for clival chordomas: 12 years of experience from a large skull base referral center. *J Neurol Surg Part B Skull Base* 2016:77–A007
- Ormond D, Wise S, Oyesiku N, Patel A, Hadjipanayis C. Endoscopic endonasal resection of clival chordomas: a case series. *J Neurol Surg B Skull Base* 2013;73:226–232
- Shkarubo AN, Koval' KV, Kadashev BA, Andreev DN, Chernov IV. Extended endoscopic endonasal posterior (transclival) approach to tumors of the clival region and ventral posterior cranial fossa. Part 3. Analysis of surgical treatment outcomes in 127 patients [in Russian]. *Vopr Neurokhir* 2018;82(03):15–28

- 32 Zoli M, Milanese L, Bonfatti R, et al. Clival chordomas: considerations after 16 years of endoscopic endonasal surgery. *J Neurosurg* 2018;128(02):329–338
- 33 Cavallo LM, Mazzatenta D, D'Avella E, et al. The management of clival chordomas: an Italian multicentric study. *J Neurosurg* 2020;135(01):93–102
- 34 Marigil M, Almeida JP, Karekezi C, de Almeida JR, Gentili F. Expanded endoscopic endonasal approach for resection of intradural chordoma: surgical and anatomic nuances: 2-dimensional operative video. *Oper Neurosurg (Hagerstown)* 2019;17(02):E66
- 35 Dehdashti AR, Karabatsou K, Ganna A, Witterick I, Gentili F. Expanded endoscopic endonasal approach for treatment of clival chordomas: early results in 12 patients. *Neurosurgery* 2008;63(02):299–307, discussion 307–309
- 36 Fraser JF, Nyquist GG, Moore N, Anand VK, Schwartz TH. Endoscopic endonasal transclival resection of chordomas: operative technique, clinical outcome, and review of the literature. *J Neurosurg* 2010;112(05):1061–1069
- 37 Fatemi N, Dusick JR, Gorgulho AA, et al. Endonasal microscopic removal of clival chordomas. *Surg Neurol* 2008;69(04):331–338
- 38 Stippler M, Gardner PA, Snyderman CH, Carrau RL, Prevedello DM, Kassam AB. Endoscopic endonasal approach for clival chordomas. *Neurosurgery* 2009;64(02):268–277, discussion 277–278
- 39 Saito K, Toda M, Tomita T, Ogawa K, Yoshida K. Surgical results of an endoscopic endonasal approach for clival chordomas. *Acta Neurochir (Wien)* 2012;154(05):879–886
- 40 Yousaf J, Afshari FT, Ahmed SK, Chavda SV, Sanghera P, Paluzzi A. Endoscopic endonasal surgery for Clival Chordomas - a single institution experience and short term outcomes. *Br J Neurosurg* 2019;33(04):388–393
- 41 Rahme RJ, Arnaout OM, Sanusi OR, Kesavabhotla K, Chandler JP. Endoscopic approach to clival chordomas: the northwestern experience. *World Neurosurg* 2018;110:e231–e238
- 42 Snyderman CH, Gardner PA. Current opinion in otolaryngology and head and neck surgery: clival chordoma and its management. *Curr Opin Otolaryngol Head Neck Surg* 2020;28(02):118–121
- 43 Beer-Furlan A, Vellutini EAS, Balsalobre L, Stamm AC. Endoscopic endonasal approach to ventral posterior fossa meningiomas: from case selection to surgical management. *Neurosurg Clin N Am* 2015;26(03):413–426
- 44 Jean WC, Felbaum DR, Anaizi A, DeKlotz TR. Endoscopic endonasal approach for transclival resection of a petroclival meningioma: a technical note. *Cureus* 2016;8(06):e641
- 45 Heiferman DM, Somasundaram A, Alvarado AJ, Zanation AM, Pittman AL, Germanwala AV. The endonasal approach for treatment of cerebral aneurysms: a critical review of the literature. *Clin Neurol Neurosurg* 2015;134:91–97
- 46 Meybodi AT, Benet A, Vigo V, et al. Assessment of the endoscopic endonasal approach to the basilar apex region for aneurysm clipping. *J Neurosurg* 2019;130(6):1937–1948
- 47 Dong X, Wang X, Shao A, Zhang J, Hong Y. Endoscopic endonasal transclival approach to ventral pontine cavernous malformation: case report. *Front Surg* 2021;8:654837
- 48 Erickson N, Siu A, Sherman JH, Gragnaniello C, Singh A, Litvack Z. Endoscopic transnasal transclival approach to a pontine cavernoma with associated developmental venous anomaly. *World Neurosurg* 2018;118:212–218
- 49 Gómez-Amador JL, Ortega-Porcayo LA, Palacios-Ortíz IJ, Perdomo-Pantoja A, Nares-López FE, Vega-Alarcón A. Endoscopic endonasal transclival resection of a ventral pontine cavernous malformation: technical case report. *J Neurosurg* 2017;127(03):553–558
- 50 Sanborn M, Storm P, Adappa N, Palmer J, Newman J, Lee J. Endoscopic, transnasal, transclival resection of a pontine cavernoma. *J Neurol Surg B Skull Base* 2012;118:212–218
- 51 Linsler S, Oertel J. Endoscopic endonasal transclival resection of a brainstem cavernoma: a detailed account of our technique and comparison with the literature. *World Neurosurg* 2015;84(06):2064–2071
- 52 Zhao B, Wei YK, Li GL, et al. Extended transsphenoidal approach for pituitary adenomas invading the anterior cranial base, cavernous sinus, and clivus: a single-center experience with 126 consecutive cases. *J Neurosurg* 2010;112(01):108–117
- 53 Liu JK, Patel J, Goldstein IM, Eloy JA. Endoscopic endonasal transclival transodontoid approach for ventral decompression of the craniovertebral junction: operative technique and nuances. *Neurosurg Focus* 2015;38(04):E17
- 54 Labib MA, Belykh E, Cavallo C, et al. The endoscopic endonasal eustachian tube anterolateral mobilization strategy: minimizing the cost of the extreme-medial approach. *J Neurosurg* 2020;134(03):831–842
- 55 Fernandez-Miranda JC, Morera VA, Snyderman CH, Gardner P. Endoscopic endonasal transclival approach to the jugular tubercle. *Neurosurgery* 2012;71(1, Suppl Operative):146–158, discussion 158–159
- 56 Karadag A, Kirgiz PG, Bozkurt B, et al. The benefits of inferolateral transtuberular route on intradural surgical exposure using the endoscopic endonasal transclival approach. *Acta Neurochir (Wien)* 2021;163(08):2141–2154
- 57 Vaz-Guimaraes Filho F, Wang EW, Snyderman CH, Gardner PA, Fernandez-Miranda JC. Endoscopic endonasal “far-medial” transclival approach: Surgical anatomy and technique. *Oper Tech Otolaryngol-Head Neck Surg* 2013;162:597–603
- 58 Sella and beyond: approaches to the clivus and posterior fossa, petrous apex, and cavernous sinus. In: *Rhinology and Skull Base Surgery*. 2014; Thieme Medical Publishers. 758–771
- 59 Kamat A, Lee JYK, Goldstein GH, et al. Reconstructive challenges in the extended endoscopic transclival approach. *J Laryngol Otol* 2015;129(05):468–472
- 60 Simal-Julian JA, Pérez de San Román-Mena L, Sanchis-Martín MR, Quiroz-Tejada A, Miranda-Lloret P, Botella-Asunción C. Septal rhinopharyngeal flap: a novel technique for skull base reconstruction after endoscopic endonasal clivectomies. *J Neurosurg* 2021;136(06):1601–1606
- 61 Iacoangeli M, Di Rienzo A, di Somma LGM, et al. Improving the endoscopic endonasal transclival approach: the importance of a precise layer by layer reconstruction. *Br J Neurosurg* 2014;28(02):241–246
- 62 Pashaev B, Danilov V, Vagapova G, et al. Failure of skull base defects reconstruction after endonasal surgery. complications, treatment options and outcomes. *J Neurol Surg Part B Skull Base* 2016
- 63 Zwagerman NT, Wang EW, Shin SS, et al. Does lumbar drainage reduce postoperative cerebrospinal fluid leak after endoscopic endonasal skull base surgery? A prospective, randomized controlled trial. *J Neurosurg* 2018;131(04):1172–1178